

VALUE OF ELECTRON-BEAM COMPUTED TOMOGRAPHY FOR THE NONINVASIVE DETECTION OF HIGH-GRADE CORONARY-ARTERY STENOSES AND OCCLUSIONS

STEPHAN ACHENBACH, M.D., WERNER MOSHAGE, M.D., DIETER ROPERS, M.D., JÖRG NOSSEN, M.D., AND WERNER G. DANIEL, M.D.

ABSTRACT

Background Reliable noninvasive assessment of coronary-artery stenoses and occlusions would constitute an advantage in the care of patients with known or suspected coronary artery disease. We investigated the accuracy of contrast-enhanced electron-beam computed tomography (CT) for the detection of high-grade coronary-artery stenoses and occlusions.

Methods Electron-beam CT was performed in 125 patients. After intravenous injection of a contrast agent, 40 cross-sectional images of the heart were acquired during inspiration, triggered by the electrocardiogram in diastole. Three-dimensional reconstructions of the heart and coronary arteries were rendered to facilitate evaluation of the images. The proximal and middle segments of the major coronary arteries were evaluated for the presence or absence of high-grade stenoses and occlusions. The results were compared with those of invasive coronary angiography in a blinded fashion.

Results Because of technical problems that impaired the quality of the images, 124 (25 percent) of the 500 coronary arteries studied (left main, left anterior descending, left circumflex, and right coronary) in a total of 125 patients were excluded from evaluation. No vessels could be evaluated in 19 patients (15 percent), and another 28 patients (22 percent) had one, two, or three vessels that could not be evaluated. In the remaining coronary arteries with adequate image quality, electron-beam CT permitted visualization of 69 of 75 high-grade stenoses and occlusions (sensitivity, 92 percent), whereas in 282 of 301 arteries, the absence of high-grade stenoses and occlusions was correctly detected (specificity, 94 percent).

Conclusions When image quality is adequate, electron-beam CT may be useful to detect or rule out high-grade coronary-artery stenoses and occlusions. (N Engl J Med 1998;339:1964-71.)

©1998, Massachusetts Medical Society.

A NNUALLY, more than 1 million coronary angiographic procedures are performed in the United States.¹ Replacing even a fraction of these diagnostic procedures with a noninvasive imaging technique would constitute an important advance in the care of patients with known or suspected coronary artery disease. Several noninvasive imaging techniques have the potential for visualization of the coronary arteries, including transthoracic and transesophageal echocardiography,²⁻⁶

synchrotron dichromography,^{7,8} and most important, magnetic resonance imaging (MRI).⁹⁻¹¹ However, because of limited spatial, temporal, or contrast resolution, none of these techniques have permitted reliable detection of coronary-artery stenoses and occlusions in a clinical setting.

Electron-beam computed tomography (CT) is a cross-sectional imaging technique with high spatial and temporal resolution; it is possible for image acquisition to be triggered by the patient's electrocardiogram. The technique is therefore well suited to cardiac imaging. It is widely used to assess coronary calcifications,¹²⁻¹⁸ and there have been preliminary reports of the use of electron-beam CT with intravenous injection of contrast agent to visualize the coronary-artery lumen.¹⁹⁻²⁵ We prospectively evaluated a group of 125 patients by both electron-beam CT and conventional coronary angiography to determine the value of the method for the noninvasive detection of high-grade stenoses and occlusions of the coronary arteries.

METHODS

Subjects

One hundred twenty-five patients (104 men and 21 women) were studied. Their mean age was 56 years (range, 23 to 82). Their average weight was 81 kg, but nine patients weighed more than 100 kg. All patients who were admitted to our institution for inpatient diagnostic coronary angiography on days on which we had access to the electron-beam CT scanner (a total of 44 days) were asked to participate in the study. Patients with coronary stents or coronary-artery bypass grafts, patients whose clinical condition was unstable, patients with atrial fibrillation, and patients with contraindications to the administration of contrast agent were excluded. All patients gave written informed consent according to institutional guidelines. Conventional invasive coronary angiography was performed by independent investigators within one week after the electron-beam CT investigation. All selected patients were included in the analysis.

Electron-Beam CT

Acquisition of Data

Electron-beam CT has previously been described in detail.^{26,27} In brief, the unique feature of this CT method is its very high imaging speed (one image can be acquired in 50 to 100 msec), which can be achieved because there is no rotating x-ray tube.

From the Department of Internal Medicine II, University of Erlangen-Nürnberg, Erlangen, Germany. Address reprint requests to Dr. Achenbach at the Medizinische Klinik II mit Poliklinik, Friedrich-Alexander-Universität Erlangen-Nürnberg, Östliche Stadtmauerstr. 29, D-91054 Erlangen, Germany.

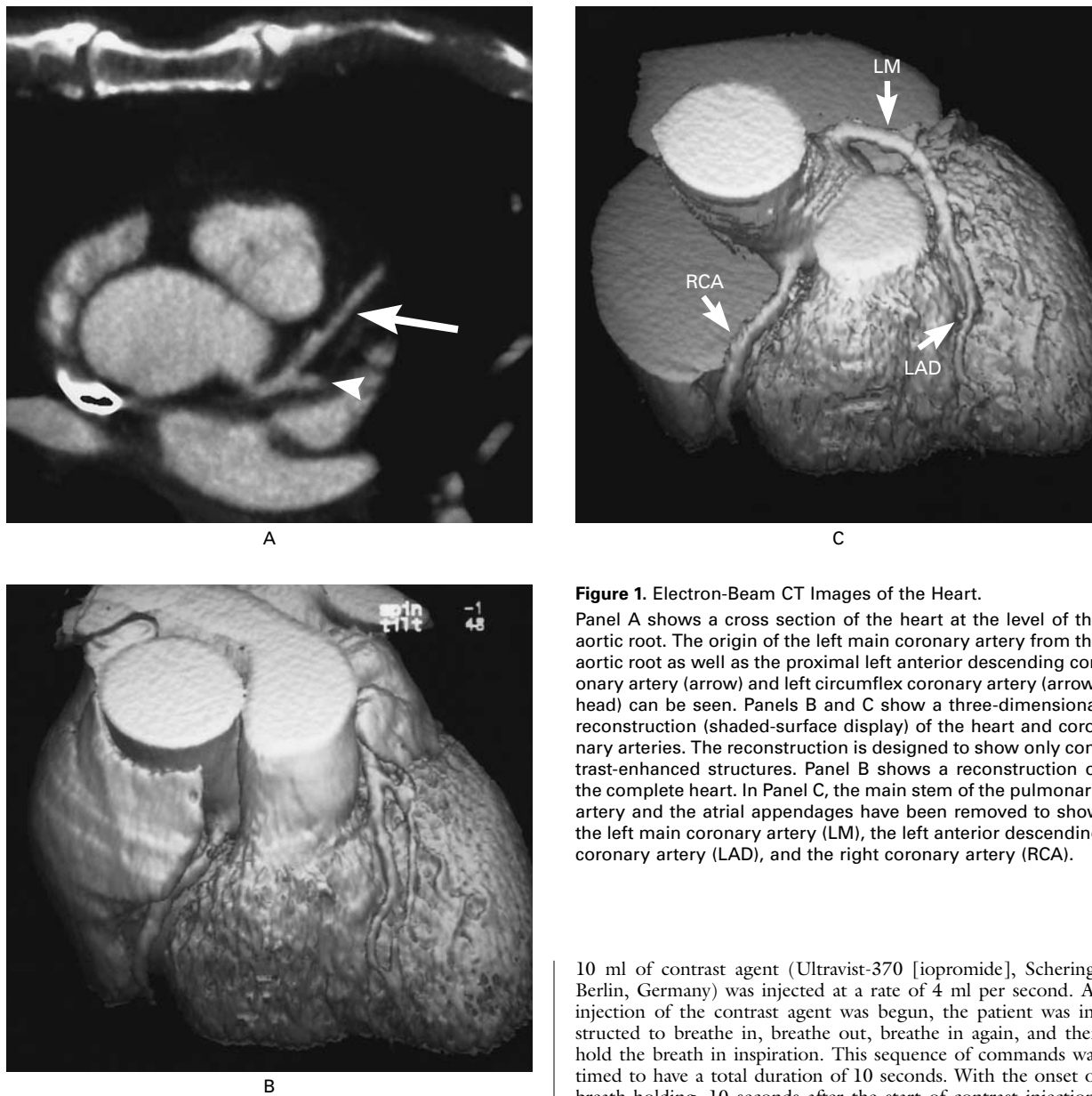


Figure 1. Electron-Beam CT Images of the Heart. Panel A shows a cross section of the heart at the level of the aortic root. The origin of the left main coronary artery from the aortic root as well as the proximal left anterior descending coronary artery (arrow) and left circumflex coronary artery (arrowhead) can be seen. Panels B and C show a three-dimensional reconstruction (shaded-surface display) of the heart and coronary arteries. The reconstruction is designed to show only contrast-enhanced structures. Panel B shows a reconstruction of the complete heart. In Panel C, the main stem of the pulmonary artery and the atrial appendages have been removed to show the left main coronary artery (LM), the left anterior descending coronary artery (LAD), and the right coronary artery (RCA).

The heart can therefore be imaged with substantially less artifact due to motion than with conventional CT scanners. In addition, scanning can be triggered by the patient's electrocardiogram. In our study, data were acquired with a C-150 XP electron-beam CT scanner (Imatron, South San Francisco, Calif.). Scanning was performed with the patient in a supine position and holding his or her breath after inspiration. Our imaging protocol consisted of three steps, as described below.

To determine the position of the heart, eight cross-sectional images of the chest (slice thickness, 7 mm; 4-mm gap between slices; field of view, 15 cm; acquisition time, 50 msec) were acquired simultaneously with the scanner in the multislice mode.

To determine exactly the transit time of the contrast agent from injection into an antecubital vein to the appearance of contrast enhancement in the aortic root and coronary arteries, a bolus of

10 ml of contrast agent (Ultravist-370 [iopromide], Schering, Berlin, Germany) was injected at a rate of 4 ml per second. As injection of the contrast agent was begun, the patient was instructed to breathe in, breathe out, breathe in again, and then hold the breath in inspiration. This sequence of commands was timed to have a total duration of 10 seconds. With the onset of breath-holding, 10 seconds after the start of contrast injection, acquisition of 10 axial cross-sectional images at the level of the aortic root was begun (single-slice mode; slice thickness, 3 mm; acquisition time, 100 msec per image). Image acquisition was triggered by the electrocardiogram, with an image being acquired after every other heartbeat at 80 percent of the RR interval. The average CT density in the aortic root was measured in each of the 10 acquired images with the scanner software. The interval between the onset of contrast injection and peak enhancement was considered to represent the transit time of the contrast agent.

In a final step, 40 axial cross-sectional images of the heart were acquired in single-slice mode. The acquisition time was 100 msec per image. With acquisition triggered by the electrocardiogram, one image was acquired after every heartbeat in diastole (at 80 percent of the cardiac cycle). The slice thickness was 3 mm, and after the acquisition of each image, the table was advanced 2 mm to generate overlapping images. The field of view was 15 cm, with an image matrix of 512 by 512, which generated a pixel size of 0.29 by 0.29 mm to make full use of the in-plane spatial resolution of the scanner (seven line pairs per centimeter).

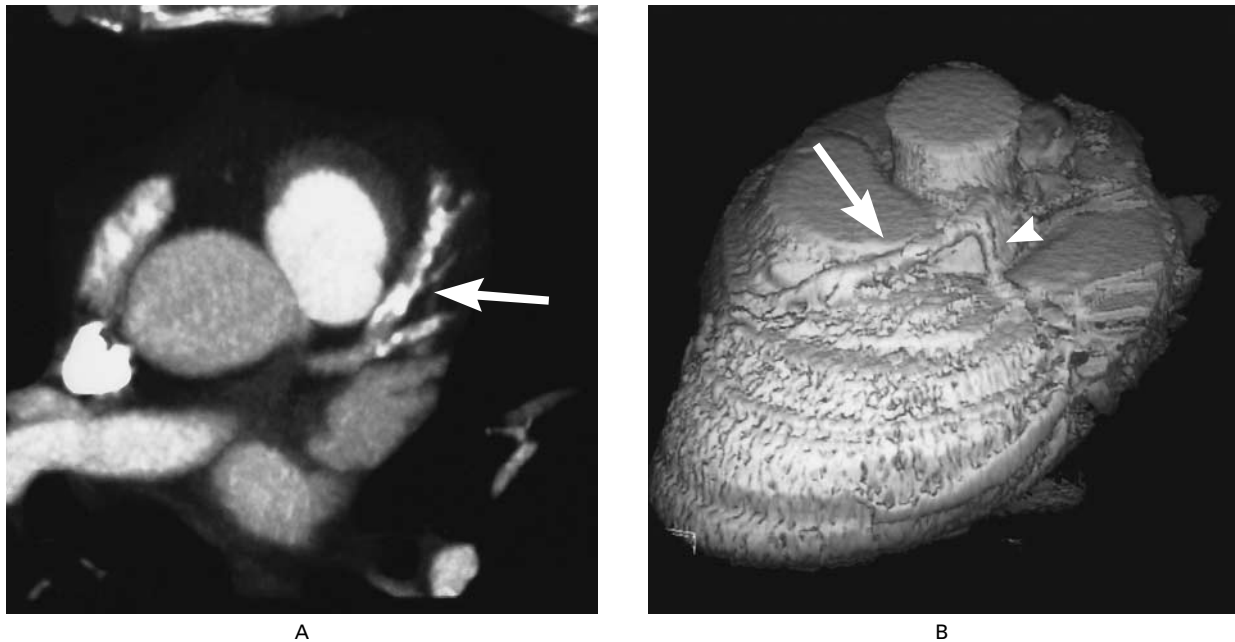


Figure 2. Frequently Observed Reasons for Inability to Evaluate Electron-Beam CT Images of the Coronary Arteries.

Panel A shows severe calcifications of the proximal left anterior descending coronary artery (arrow). In Panel B, artifacts of respiration render the left anterior descending coronary artery (arrow), left circumflex coronary artery (arrowhead), and right coronary artery (not seen from this angle) impossible to evaluate.

Images were acquired with the patient holding his or her breath after inspiration and with breathing commands identical to those used for the determination of the transit time of the contrast agent. The scanner permits the acquisition of one image per cardiac cycle for heart rates up to 120 beats per minute. With heart rates between 44 and 104 beats per minute (mean, 69) during acquisition of the images, the duration of breath-holding was 23 to 54 seconds (mean, 35). Between 120 and 160 ml of contrast agent was injected intravenously at a rate of 4 ml per second. A delay corresponding to the individually determined transit time of the contrast agent was maintained between the initiation of injection of the contrast agent and the acquisition of the first image. The radiation dose was estimated to be less than 11 mSv.^{12,28}

Evaluation of Data

The images obtained by electron-beam CT were independently evaluated by two investigators without knowledge of the findings on the patients' coronary angiograms. The image data were transferred to an off-line workstation (MagicView, Siemens, Erlangen, Germany). The cross-sectional images were screened for artifacts caused by motion and for calcifications of the coronary arteries. Calcifications were rated as too severe to permit further evaluation if a calcified plaque occupied more than half the diameter of the artery in two consecutive images. Manual segmentation of the images was performed on an image-by-image basis to eliminate all structures that would obstruct the view of the coronary arteries, such as the chest wall, pulmonary vessels, and atrial appendages (Fig. 1). Subsequently, three-dimensional reconstructions of the heart and coronary arteries were rendered by a shaded-surface display technique. A lower threshold of 80 Hounsfield units was used for the reconstruction in all patients to visualize selectively the contrast-enhanced lumina of the coronary arteries, while ignoring the vessel wall and surrounding connective tissue (Fig. 1).¹⁹ Three-dimensional reconstructions were rendered interactively from at least six angles (equivalent to posteroanterior, left

anterior oblique, and right anterior oblique projections, each in at least two craniocaudal angulations). If necessary, reconstructions were rendered from additional angles to depict all coronary segments from two orthogonal directions.

On the basis of the original cross-sectional images and the three-dimensional reconstructions, both investigators independently rated the left main coronary artery (segment 5 according to the system of the American Heart Association²⁹) and the proximal and middle segments of the left anterior descending coronary artery (segments 6 and 7 and the first half of segment 8), the left circumflex coronary artery (segments 11 and 13), and the right coronary artery (segments 1 and 2) as being occluded or having a high-grade stenosis (more than 75 percent reduction in diameter), showing neither high-grade stenosis nor occlusion, or being impossible to evaluate. The side branches and the distal segments of the coronary arteries were not included in the evaluation. Determination of the severity of stenosis was based on visual estimation of both the axial cross sections and the three-dimensional reconstructions. In the reconstructions, the severity of the lesion was determined in the projection that showed the highest degree of stenosis. Cohen's kappa³⁰ was calculated to determine agreement between observers on which of three categories was applicable (status impossible to evaluate, high-grade stenosis or occlusion absent, and high-grade stenosis or occlusion present).

Coronary Angiography

In all patients, coronary angiography was performed by the transfemoral Judkins approach. Angiograms were documented on cine film and evaluated by two cardiologists who were independent of the electron-beam CT team. Reductions in diameter of more than 75 percent were considered to represent high-grade stenoses. In cases of disagreement between the two readers, agreement was achieved in a joint reading. Cohen's kappa was calculated to determine variability between observers, with regard to the same categories as for electron-beam CT (status impossible

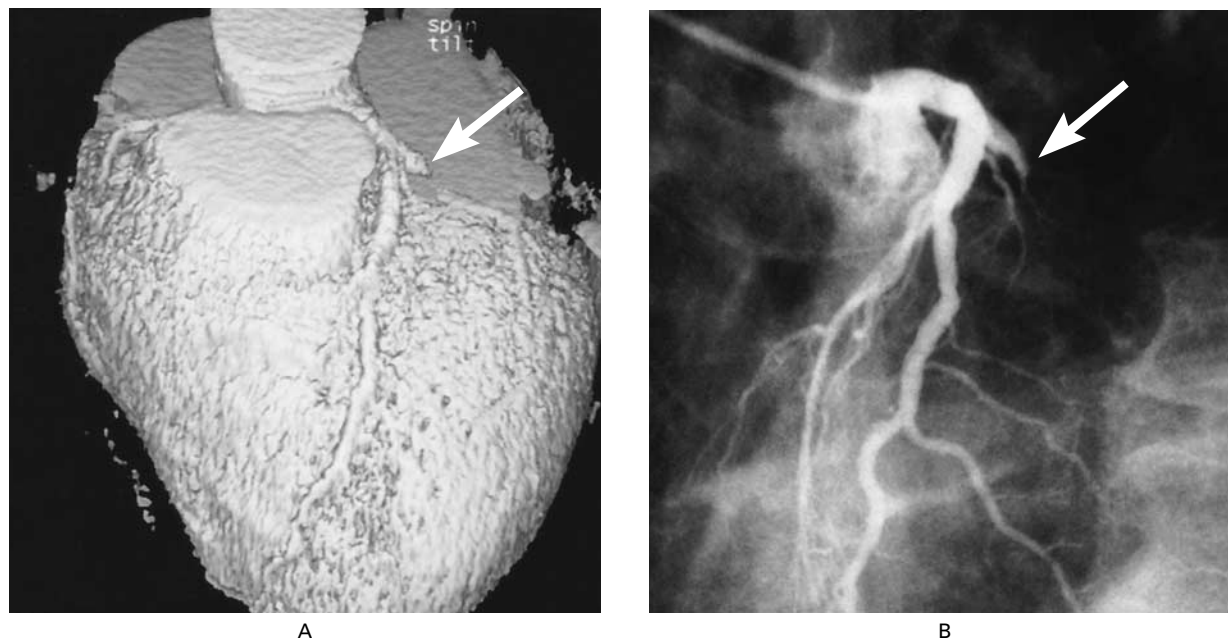


Figure 3. Cardiac Images of a 56-Year-Old Patient with a Complete Occlusion of the Left Circumflex Coronary Artery (Arrow) According to Electron-Beam CT (Panel A) and Coronary Angiography (Panel B).

to evaluate, high-grade stenosis or occlusion absent, and high-grade stenosis or occlusion present).

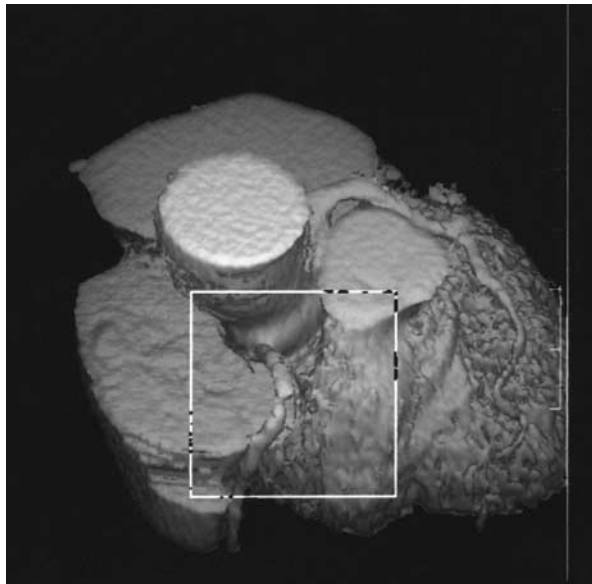
RESULTS

In all the patients, electron-beam CT was performed without complications. The mean time needed for the investigation was 18 ± 3 minutes per patient, including all preparations for scanning. Of the 500 coronary arteries (left main, left anterior descending, left circumflex, and right coronary artery in 125 patients), 124 were considered impossible to evaluate because of technical problems. The main reasons for impaired image quality were artifacts of respiration (40 vessels) and severe calcifications (33 vessels) (Fig. 2), as well as artifacts of movement of the left circumflex coronary artery (11 vessels) and the right coronary artery (14 vessels). Other reasons included reduced signal-to-noise ratio (12 vessels), superposition of veins (5 vessels), malpositioning of the imaging volume (5 vessels), and a very small arterial lumen (4 vessels). In 11 patients, one coronary artery could not be evaluated; in 14 patients, two arteries could not be evaluated; and in 3 patients, three vessels could not be evaluated. In 19 patients (15 percent), the quality of the image was too poor for any of the four arteries to be evaluated. The reduction in image quality in these patients was caused by artifacts of respiration in eight, severe calcifications in five, reduced signal-to-noise ratio in three, and more than one of these factors in three.

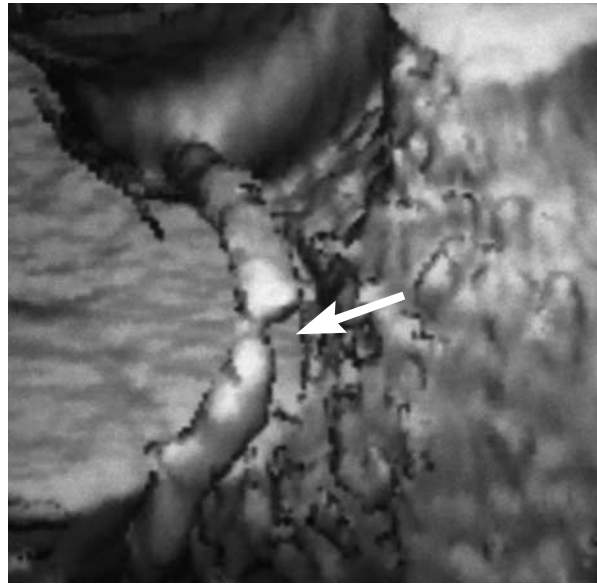
The left main coronary artery could be evaluated in 105 patients (84 percent), the left anterior descending coronary artery in 100 patients (80 percent), the left circumflex coronary artery in 83 patients (66 percent), and the right coronary artery in 88 patients (70 percent).

With the 124 coronary arteries that were graded as impossible to evaluate excluded from the analysis, 41 of 42 substantial lesions (high-grade stenoses and occlusions) of the left anterior descending coronary artery, 14 of 18 substantial lesions of the left circumflex coronary artery, and 14 of 15 substantial lesions of the right coronary artery were correctly detected by electron-beam CT (Fig. 3 and 4). In the arteries that could be evaluated, the absence of high-grade stenosis or complete occlusion was correctly determined in 104 of 105 cases for the left main coronary artery, 51 of 58 cases for the left anterior descending coronary artery, 57 of 65 cases for the left circumflex coronary artery, and 70 of 73 cases for the right coronary artery (Table 1). These numbers correspond to a sensitivity of 92 percent, a specificity of 94 percent, a positive predictive value of 78 percent, and a negative predictive value of 98 percent for the detection of substantial coronary lesions in the arteries that could be evaluated.

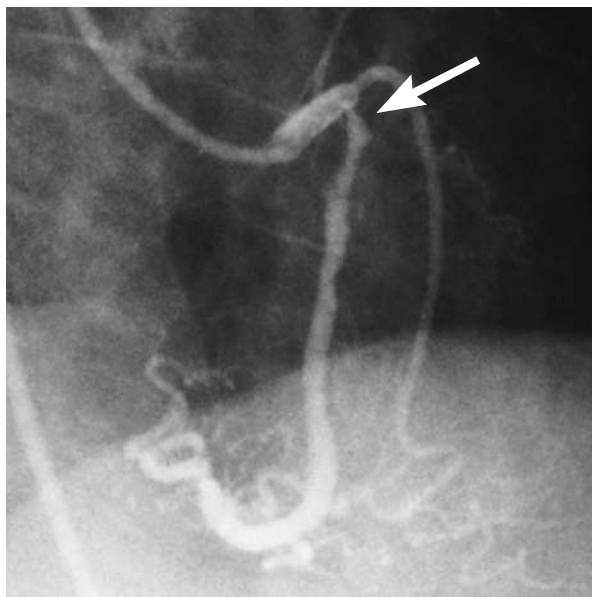
Whether a vessel could be evaluated by electron-beam CT was not associated with the angiographic results for that vessel (Table 2). Of the 376 vessels that could be evaluated by electron-beam CT, 75



A



B



C

Figure 4. Cardiac Images of an 81-Year-Old Patient with a High-Grade Stenosis of the Right Coronary Artery (Arrow) According to Electron-Beam CT (Panels A and B) and Coronary Angiography (Panel C).

(20 percent) had a high-grade stenosis or occlusion on angiography; of the 124 arteries that could not be evaluated by electron-beam CT, 24 (19 percent) had a high-grade stenosis or occlusion on angiography.

Overall, when arteries that could not be evaluated were included, electron-beam CT permitted visualization of 69 of the 99 high-grade coronary-artery stenoses and occlusions that were detected by angiography in the group of patients we investigated. Of the 401 coronary arteries that were documented by

angiography to be free of high-grade lesions, 282 were correctly identified by electron-beam CT.

Interobserver agreement was achieved for 453 of the 500 coronary arteries (91 percent). Cohen's kappa was 0.82, indicating close agreement between observers. Disagreement concerned mainly the quality of the images: in 31 of the 47 coronary vessels with discrepant readings, one of the two observers considered image quality to be too poor for evaluation. With conventional angiography, agreement between the observers was achieved in 96 percent of cases without joint reading, and Cohen's kappa was 0.90.

DISCUSSION

Because of its high spatial and temporal resolution as well as the fact that image acquisition can be triggered by the electrocardiogram, electron-beam CT is well suited for cardiac imaging. In a clinical setting, this method, which has also been called "ultrafast CT" or "cine CT," has been applied principally to visualize and quantify coronary calcifications¹²⁻¹⁷ and to evaluate cardiac function.³¹ However, preliminary reports have indicated the potential of the method, after intravenous injection of contrast agent, to visualize the coronary-artery lumen^{19,20} and to detect stenoses noninvasively.²¹⁻²⁵ In our investigation, we found a high sensitivity and specificity, as well as a very high negative predictive value of 98 percent, for the detection of complete occlusions and high-grade stenoses

TABLE 1. ACCURACY OF ELECTRON-BEAM CT FOR THE DETECTION OF HIGH-GRADE STENOSES AND OCCLUSIONS OF THE CORONARY ARTERIES.

CORONARY ARTERY	EVALUATION POSSIBLE	SENSITIVITY*	SPECIFICITY*
	% (no. of arteries/total no.)		
Total	75 (376/500)	92 (69/75)	94 (282/301)
Left main	84 (105/125)	0 (0/0)	99 (104/105)
Left anterior descending	80 (100/125)	98 (41/42)	88 (51/58)
Left circumflex	66 (83/125)	78 (14/18)	88 (57/65)
Right	70 (88/125)	93 (14/15)	96 (70/73)

*Sensitivity and specificity were calculated only for the arteries that could be evaluated.

TABLE 2. RELATION BETWEEN ANGIOGRAPHIC STATUS OF THE CORONARY ARTERIES AND RESULTS OF ELECTRON-BEAM CT.

RESULTS OF ELECTRON-BEAM CT	ANGIOGRAPHIC STATUS		TOTAL
	ABSENCE OF HIGH-GRADE STENOSIS OR OCCLUSION	PRESENCE OF HIGH-GRADE STENOSIS OR OCCLUSION	
Absence of high-grade stenosis or occlusion	282	6	288
Presence of high-grade stenosis or occlusion	19	69	88
Could not be evaluated	100	24	124
Total	401	99	500

of the coronary arteries, provided that sufficiently good image quality could be obtained. In the vessels that could be evaluated, the number of false negative results for stenoses was small (92 percent sensitivity). Most stenoses that were missed were located in the left circumflex and right coronary arteries. These vessels are perpendicular to the imaging plane and are therefore visualized with lower spatial resolution than those oriented parallel to the imaging plane. As in earlier, smaller studies, most false positive results were for stenoses in smaller vessels²³ (again, the left circumflex coronary artery in most cases).

The main drawback of electron-beam CT currently seems to be that 25 percent of all coronary segments had to be excluded from evaluation because of inadequate image quality. Because of their position in the coronary groove, the left circumflex and right coronary arteries have more rapid diastolic

motion than the left anterior descending coronary artery. The motion is caused mainly by atrial contraction during end-diastole. In addition, the interpretation of results for all coronary arteries may be compromised by artifacts of respiration if patients are unable to obey the breath-holding commands. Although mildly calcified vessels can be evaluated, extensive calcifications are a frequent reason for false negative^{23,25} and false positive²² results. We therefore excluded all arteries with more than mild calcifications from evaluation. Mistriggering of single cross sections (from premature beats, for example) was not observed as frequently as previously reported.²²

Before the method is applied on a broad clinical scale, the number of studies that cannot be evaluated will have to be reduced. To do this, it will be necessary to ensure, for example, that through more careful instruction and preparation patients hold their breath for the full scanning period. Alternatively, the heart rate may be medically increased to shorten the overall image-acquisition time. Furthermore, choosing different imaging planes could increase spatial resolution in the vessel segments that are perpendicular to the axial imaging plane we used in the present study (the middle right coronary artery and the left circumflex coronary artery).²³ Further reducing the image-acquisition time or optimizing the time interval in the cardiac cycle that is used for image acquisition would probably diminish artifacts of motion. Higher spatial resolution of the scanner might improve the detection of short lesions and of stenoses in small arteries. It might also permit the development of image-processing techniques to subtract calcified plaques, something that is currently not possible, because of the overlap of density values between calcifications and contrast-enhanced vessel lumen.

Our evaluation was limited to the proximal and middle segments of the major coronary arteries. Distal segments and side branches were excluded because their small diameters do not permit reliable imaging with the spatial resolution the scanner currently provides (seven line pairs per centimeter in the imaging plane), and partial-volume effects would lead to an unacceptably high number of false positive results. However, since lesions in distal segments and side branches are rarely the target of catheter intervention or bypass revascularization, the fact that electron-beam CT imaging is limited to segments of larger diameter does not mean that the technique may not be clinically useful. Similarly, no attempt was made to differentiate between high-grade stenoses and complete occlusions of coronary arteries. In electron-beam CT, the partial-volume effect can cause a very tight stenosis to appear to be a complete occlusion of the vessel lumen. Consequently, it may be impossible to decide whether such a lesion represents a high-grade stenosis or a complete occlusion with filling of the distal segment by collateral flow.

For clinical applications, however, mistaking complete occlusions for high-grade stenoses would in most cases be irrelevant, since both conditions usually require further invasive testing.

The accuracy of electron-beam CT for the diagnosis of high-grade stenoses and occlusions of the coronary arteries seems to be superior to that of other noninvasive techniques. Echocardiography permits the assessment of only the most proximal segments of the coronary arteries, and the technique is unreliable for identifying coronary lesions. Dichromatic synchrotron angiography has not yet been evaluated on a broad scale. Magnetic resonance coronary-angiography techniques are evolving rapidly. As compared with electron-beam CT, they have the advantage of requiring no exposure to radiation and, in most cases, no injection of contrast agent. However, the spatial and temporal resolution of currently available MRI techniques³²⁻³⁷ is inferior to that of electron-beam CT, and except for respiratory-gated acquisitions,^{36,37} the necessary respiratory maneuvers require a high degree of cooperation from patients.³²⁻³⁵ The reported accuracy of MRI protocols that have been proposed for the detection of coronary-artery stenoses varies widely, from 38 to 90 percent,³²⁻³⁷ and (with the possible exception of visualizing the course of anomalous coronary arteries³⁸⁻⁴⁰) magnetic resonance angiography is currently considered an investigational technique.^{10,11,40,41}

The high negative predictive value of electron-beam CT for the detection of high-grade stenoses in patients with adequate image quality may make this method a clinically useful test. Since we found that the results of electron-beam CT could be completely evaluated in 62 percent of all patients, and that whether or not they could be evaluated was not related to the angiographic status of the arteries, it can be calculated that up to two thirds of the coronary angiographic procedures that demonstrate normal coronary arteries could currently be averted by the use of this noninvasive test. Further research must be directed toward reducing the number of nondiagnostic studies. Once this goal has been achieved, electron-beam CT may become a useful tool to rule out high-grade coronary-artery stenoses or occlusions in, for example, patients with a low likelihood of obstructive coronary disease, and also in patients who have undergone balloon angioplasty or bypass grafting. In this way, a substantial number of the invasive coronary angiographic studies that have negative results, which constitute up to 20 percent of all studies performed,⁴² could be replaced by noninvasive outpatient examinations.

REFERENCES

- 1993 Heart and stroke facts statistics. Dallas: American Heart Association, 1993:8.
- Hozumi T, Yoshida K, Ogata Y, et al. Noninvasive assessment of significant left anterior descending coronary artery stenosis by coronary flow velocity reserve with transthoracic color Doppler echocardiography. *Circulation* 1998;97:1557-62.
- Feigenbaum H. Transthoracic ultrasonic visualization of coronary atherosclerosis. *J Am Soc Echocardiogr* 1989;2:253-8.
- Tardif JC, Vannan MA, Taylor K, Schwartz SL, Pandian NG. Delineation of extended lengths of coronary arteries by multiplane transesophageal echocardiography. *J Am Coll Cardiol* 1994;24:909-19.
- Caiati C, Aragona P, Iliceto S, Rizzon P. Improved detection of proximal left anterior descending coronary artery stenosis after intravenous injection of a lung-crossing contrast agent: a transesophageal Doppler echocardiographic study. *J Am Coll Cardiol* 1996;27:1413-21.
- Mulvagh SL, Foley DA, Aeschbacher BC, Klarich KK, Seward JB. Second harmonic imaging of an intravenously administered echocardiographic contrast agent: visualization of coronary arteries and measurement of coronary blood flow. *J Am Coll Cardiol* 1996;27:1519-25.
- Rubenstein E, Brown GS, Chapman D, et al. Synchrotron radiation coronary angiography in humans. In: Chance B, Deisenhofer J, Ebashi S, et al., eds. *Synchrotron radiation in the biosciences*. New York: Oxford University Press, 1994:639-50.
- Hamm CW, Meinertz T, Dix WR, et al. Intravenous coronary angiography with dichromography using synchrotron radiation. *Herz* 1996;21:127-31.
- Manning WJ, Edelman RR. Magnetic resonance coronary angiography. *Magn Reson Q* 1993;9:131-51.
- Taylor AM, Pennell DJ. Recent advances in cardiac magnetic resonance imaging. *Curr Opin Cardiol* 1996;11:635-42.
- van der Wall EE, van Ruge FP, Vliegen HW, Reiber JH, de Roos A, Brusckhe AV. Ischemic heart disease: value of MR techniques. *Int J Card Imaging* 1997;13:79-89.
- Agatston AS, Janowitz WR, Hildner FJ, Zusmer NR, Viamonte M Jr, Detrano R. Quantification of coronary artery calcium using ultrafast computed tomography. *J Am Coll Cardiol* 1990;15:827-32.
- Ultrafast CT for coronary calcification. *Lancet* 1991;337:1449-50.
- Breen JF, Sheedy PF II, Schwartz RS, et al. Coronary artery calcification detected with ultrafast CT as an indication of coronary artery disease. *Radiology* 1992;185:435-9.
- Budoff MJ, Georgiou D, Brody A, et al. Ultrafast computed tomography as a diagnostic modality in the detection of coronary artery disease: a multicenter study. *Circulation* 1996;93:898-904.
- Arad Y, Spadaro LA, Goodman K, et al. Predictive value of electron beam computed tomography of the coronary arteries: 19-month follow-up of 1173 asymptomatic subjects. *Circulation* 1996;93:1951-3.
- Detrano R, Hsiai T, Wang S, et al. Prognostic value of coronary calcification and angiographic stenoses in patients undergoing coronary angiography. *J Am Coll Cardiol* 1996;27:285-90.
- Rumberger JA, Sheedy PF II, Breen JF, Fitzpatrick LA, Schwartz RS. Electron beam computed tomography and coronary artery disease: scanning for coronary artery calcification. *Mayo Clin Proc* 1996;71:369-77.
- Moshage WE, Achenbach S, Seese B, Bachmann K, Kirchengoerg M. Coronary artery stenoses: three-dimensional imaging with electrocardiographically triggered, contrast agent-enhanced, electron-beam CT. *Radiology* 1995;196:707-14.
- Chernoff DM, Ritchie CJ, Higgins CB. Evaluation of electron beam CT coronary angiography in healthy subjects. *AJR Am J Roentgenol* 1997;169:93-9.
- Budoff MJ, Oudiz RJ, Zalace CP, et al. Intravenous three dimensional coronary angiography using contrast enhanced electron beam computed tomography. *J Am Coll Cardiol* 1997;29:Suppl A:393A. abstract.
- Nakanishi T, Ito K, Imazu M, Yamakido M. Evaluation of coronary artery stenoses using electron-beam CT and multiplanar reformation. *J Comput Assist Tomogr* 1997;21:121-7.
- Schmermund A, Rensing BJ, Sheedy PF, Bell MR, Rumberger JA. Intravenous electron-beam computed tomographic coronary angiography for segmental analysis of coronary artery stenoses. *J Am Coll Cardiol* 1998;31:1547-54.
- Reddy GP, Chernoff DM, Siripornpitak S, Adams JR, Outtrim RA, Higgins CB. Assessment of coronary artery stenoses with contrast-enhanced electron-beam CT and axial reconstructions. *Radiology* 1997;205:Suppl:459. abstract.
- Achenbach S, Moshage W, Bachmann K. Detection of high-grade restenosis after PTCA using contrast-enhanced electron beam CT. *Circulation* 1997;96:2785-8.
- Boyd D, Gould RG, Quinn J, Sparks R, Stanley R, Hermannsfeldt W. A proposed cardiac 3-d densitometer for easy detection and evaluation of heart disease. *IEEE Trans Nucl Sci* 1979;26:2724-7.
- Gould RG. Principles of ultrafast computed tomography: historical aspects, mechanism of action, and scanner characteristics. In: Stanford W, Rumberger JA, eds. *Ultrafast computed tomography in cardiac imaging: principles and practice*. Mount Kisco, N.Y.: Futura Publishing, 1992:1-16.

28. Stanford W, Thompson BH, Weiss RM. Coronary artery calcification: clinical significance and current methods of detection. *AJR Am J Roentgenol* 1993;161:1139-46.
29. A reporting system on patients evaluated for coronary artery disease: report of the Ad Hoc Committee for Grading of Coronary Artery Disease, Council on Cardiovascular Surgery, American Heart Association. *Circulation* 1975;51:Suppl:5-40.
30. Cohen J. A coefficient for agreement on nominal scales. *Educ Psychol Meas* 1960;20:37-46.
31. Rumberger JA. Quantifying left ventricular regional and global systolic function using ultrafast computed tomography. *Am J Cardiac Imaging* 1991;5:29-37.
32. Manning WJ, Li W, Edelman RR. A preliminary report comparing magnetic resonance coronary angiography with conventional angiography. *N Engl J Med* 1993;328:828-32. [Erratum, *N Engl J Med* 1994;330:152.]
33. Post JC, van Rossum AC, Hofman MB, Valk J, Visser CA. Three-dimensional respiratory-gated MR angiography of coronary arteries: comparison with conventional coronary angiography. *AJR Am J Roentgenol* 1996;166:1399-404.
34. Pennell DJ, Bogren HG, Keegan J, Firmin DN, Underwood SR. Assessment of coronary artery stenosis by magnetic resonance imaging. *Heart* 1996;75:127-33.
35. Mohiaddin RH, Bogren HG, Lazim F, et al. Magnetic resonance coronary angiography in heart transplant recipients. *Coron Artery Dis* 1996;7:591-7.
36. Kessler W, Achenbach S, Moshage W, et al. Usefulness of respiratory gated magnetic resonance coronary angiography in assessing narrowings > or = 50% in diameter in native coronary arteries and in aortocoronary bypass conduits. *Am J Cardiol* 1997;80:989-93.
37. Muller MF, Fleisch M, Kroeker R, Chatterjee T, Meier B, Vock P. Proximal coronary artery stenosis: three-dimensional MRI with fat saturation and navigator echo. *J Magn Reson Imaging* 1997;7:644-51.
38. McConnell MV, Ganz P, Selwyn AP, Li W, Edelman RR, Manning WJ. Identification of anomalous coronary arteries and their anatomic course by magnetic resonance coronary angiography. *Circulation* 1995;92:3158-62.
39. Post JC, van Rossum AC, Bronzwaer JGF, et al. Magnetic resonance angiography of anomalous coronary arteries: a new gold standard for delineating the proximal course? *Circulation* 1995;92:3163-71.
40. Task Force of the European Society of Cardiology, Association of European Paediatric Cardiologists. The clinical role of magnetic resonance in cardiovascular disease. *Eur Heart J* 1998;19:19-39.
41. Duerinckx AJ. MR angiography of the coronary arteries. *Top Magn Reson Imaging* 1995;7:267-85.
42. Johnson LW, Lozner EC, Johnson S, et al. Coronary arteriography 1984-1987: a report of the Registry of the Society for Cardiac Angiography and Interventions. I. Results and complications. *Cathet Cardiovasc Diagn* 1989;17:5-10.